

Nonlinear thermal buckling behavior of functionally graded plates using an efficient sinusoidal shear deformation theory

Rabbab Bachir Bouiadjra^{1,2}, E.A. Adda Bedia² and Abdelouahed Tounsi^{*2,3}

¹Faculté d'Architecture & de Génie Civil, Département de Génie Civil, Université Sciences et de la Technologie d'Oran, Algeria

²Laboratoire des Matériaux et Hydrologie, Faculté de Technologie, Université de Sidi Bel Abbes, Algeria

³Laboratoire des Structures et Matériaux Avancés dans le Génie Civil et Travaux Publics, Université de Sidi Bel Abbes, Faculté de Technologie, Département de Génie Civil, Algeria

(Received August 5, 2012, Revised October 18, 2013, Accepted October 26, 2013)

Abstract. Nonlinear behavior of functionally graded material (FGM) plates under thermal loads is investigated here using an efficient sinusoidal shear deformation theory. The displacement field is chosen based on assumptions that the in-plane and transverse displacements consist of bending and shear components, and the shear components of in-plane displacements give rise to the sinusoidal distribution of transverse shear stress through the thickness in such a way that shear stresses vanish on the plate surfaces. Therefore, there is no need to use shear correction factor. Unlike the conventional sinusoidal shear deformation theory, the proposed efficient sinusoidal shear deformation theory contains only four unknowns. The material is graded in the thickness direction and a simple power law based on the rule of mixture is used to estimate the effective material properties. The neutral surface position for such FGM plates is determined and the sinusoidal shear deformation theory based on exact neutral surface position is employed here. There is no stretching–bending coupling effect in the neutral surface-based formulation, and consequently, the governing equations and boundary conditions of functionally graded plates based on neutral surface have the simple forms as those of isotropic plates. The non-linear strain–displacement relations are also taken into consideration. The thermal loads are assumed as uniform, linear and non-linear temperature rises across the thickness direction. Closed-form solutions are presented to calculate the critical buckling temperature, which are useful for engineers in design. Numerical results are presented for the present efficient sinusoidal shear deformation theory, demonstrating its importance and accuracy in comparison to other theories.

Keywords: functional composites; thermal properties; buckling; plate theory; neutral surface position

1. Introduction

The increased applications of advanced composite materials in structural members have stimulated interest in the accurate prediction of the response characteristics of functionally graded (FG) plates used in situations where large temperature gradients are encountered. Functionally graded materials (FGMs) are designed so that material properties vary smoothly and continuously

*Corresponding author, Professor, E-mail: tou_abdel@yahoo.com

through the thickness from the surface of a ceramic exposed to high temperature to that of a metal on the other surface. The mechanical properties are graded in the thickness direction according to volume fraction power law distribution. Since the main applications of FGMs have been in high temperature environments, most of the research on FGMs has been restricted to thermal stress analysis, thermal buckling, fracture mechanics and optimization.

A number of investigations dealing with thermal buckling of functionally graded plate (FGP) had been proposed in the published literature. The nonhomogeneous mechanical properties of the FGP, graded through the thickness, are described by a power function of the thickness variable. Equilibrium equations of a rectangular FGP under thermal loads based on higher order theory were derived by Javaheri and Eslami (2002a). The system of fundamental partial differential equations was established by using the variational method. The derived equilibrium and stability equations for FGPs are identical to the equations for laminated composite plates. A buckling analysis of an FGP under four types of thermal loads was presented. Na and Kim (2004) investigated the three dimensional thermomechanical buckling of an FGP composed of ceramic, FGM, and metal layers. The thermal buckling behaviors of FGM composite structures due to FGM thickness ratios, volume fraction distributions, and system geometric parameters were analyzed. The thermal buckling of circular functionally graded plate was studied by Najafizadeh and Heydaru (2004). By assuming that the material properties vary as a power form of the thickness coordinate variable z and using the variational method, the buckling of a functionally graded circular plate under various thermal loads was analyzed. Equilibrium equations of a thick rectangular FGP under thermal loads were derived by Lanhe (2004). Thermal loading of uniform temperature rise and gradient through the thickness was considered. The influences of the volume fraction index and the transverse shear on the thermal buckling temperature were discussed. Bouazza *et al.* (2010) investigated the thermoelastic buckling of FGP using first shear plate theory. Effects of changing plate characteristics, material composition and volume fraction of constituent materials on the critical temperature difference of FGP with simply supported edges are also investigated. Shariat and Eslami (2005) presented the thermal buckling analysis of rectangular FGPs with geometrical imperfections based on the classical plate theory. Three types of thermal loading as uniform temperature rise, nonlinear temperature rise through the thickness and axial temperature rise were considered. The thermal buckling of a simply supported skew FGP was investigated by Ganapathi (2006) based on the first-order theory. Linear and nonlinear temperature rise across the thickness were taken into account. The effects of aspect and thickness ratios, gradient index and skew angle on the critical buckling temperature difference are studied. Morimoto *et al.* (2006) presented the thermal buckling analysis of rectangular FGPs subjected to partial heating in a plane and uniform temperature rise through its thickness. The FGM properties of linear thermal expansion and Young's modulus are changed individually in the thickness direction of the plate with the power law. The effects of material inhomogeneity, aspect ratio, and heated region on the critical buckling temperatures are examined. Thermal buckling of an FGP under the combined effect of elevated temperature and aerodynamic loading was studied by Ibrahim *et al.* (2007). It is found that the temperature increase has an adverse effect on the FGP flutter characteristics through decreasing the critical dynamic pressure. Decreasing the volume fraction enhances the flutter characteristic. Sohn and Kim (2008) dealt with the stabilities of FG panels subjected to combined thermal and aerodynamic loads. The first-order theory was used to simulate supersonic aerodynamic loads acting on the panels. Matsunaga (2009) presented a higher order deformation theory for thermal buckling of FGPs. By using the method of power series expansion of displacement components, a set of fundamental equations of rectangular FGPs was derived. Kazerouni *et al.* (2010) presented

thermal buckling analysis of thin functionally graded plates under two cases of thermal loadings as the uniform and non-linear temperature rise cases. Recently, Kettaf *et al.* (2013) investigated the thermal buckling behavior of functionally graded sandwich plates using a new hyperbolic displacement model.

Neutral surface of functionally graded plate may not coincide with its geometric mid-surface, because of the material property variation through the thickness, leading to bending-extension coupling. Therefore, stretching and bending deformations of FG plate are coupled. Some researchers (Morimoto *et al.* 2006, Abrate 2008, Zhang and Zhou 2008, Saidi and Jomehzadeh 2009) have shown that there is no stretching-bending coupling in constitutive equations if the reference surface is properly selected. Recently, Bodaghi and Saidi (2011) investigated the buckling of thin FG plates under non-uniform in-plane loading in the framework of the classical thin plate theory. They used the neutral surface concept and showed that the stability equations based on the classical plate theory reduced to the single buckling equation which can be solved by using the power series method straightforwardly.

This paper aims to develop an efficient sinusoidal shear deformation theory based on exact position of neutral surface for thermal buckling analysis of FG plates. This theory is based on assumption that the in-plane and transverse displacements consist of bending and shear components in which the bending components do not contribute toward shear forces and, likewise, the shear components do not contribute toward bending moments. Unlike the conventional sinusoidal shear deformation theory (Zenkour and Mashat 2010), the proposed sinusoidal shear deformation theory contains four unknowns. The material properties are graded in the thickness direction according to the power-law distribution in terms of volume fractions of the constituents of the material. The effective material properties are estimated using a simple power law based on rule of mixture. Since, the material properties of FG plate vary through the thickness direction, the neutral plane of such plate may not coincide with its geometric middle plane (Yahoobi and Feraidoon 2010). In addition, Zhang and Zhou (2008), Ould Larbi *et al.* (2013), Bouremana *et al.* (2013), Khalfi *et al.* (2013), Bousahla *et al.* (2013) show that the stretching – bending coupling in the constitutive equations of an FG plate does not exist when the coordinate system is located at the physical neutral surface of the plate. Therefore, the governing equations for the FG plate can be simplified. Based on the present theory and the exact position of neutral surface together with the principle of virtual work, the governing equations of the functionally graded plates are obtained. The thermal loads are assumed to be uniform, linear and non-linear distribution through the thickness. The results are compared and validated with the results of previous works which are available in the literature.

2. Problem formulation

Consider a rectangular plate made of FGMs of thickness h , length a , and width b made by mixing two distinct materials (metal and ceramic) is studied here. The coordinates x , y are along the in-plane directions and z is along the thickness direction. The top surface material is ceramic rich and the bottom surface material is metal rich. For such plates, the neutral surface may not coincide with its geometric mid-surface. The applied compressive force may be assumed to act at the mid-surface of the plate for all the practical purposes, but the in-plane stress resultants act along the neutral surface. The noncoincidence of line of action of stress resultant and applied compressive force results in a couple as schematically shown in Fig. 1. The present study attempts

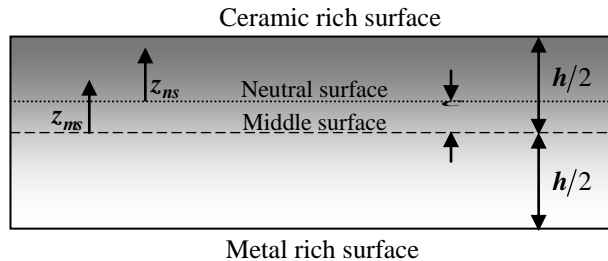


Fig. 1 The position of middle surface and neutral surface for a functionally graded plate

to investigate the position of neutral surface and the deflection characteristics under in-plane loads.

Here, two different datum planes are considered for the measurement of z , namely, z_{ms} and z_{ns} measured from the middle surface, and the neutral surface of the plate, respectively (Fig. 1). The volume-fraction of ceramic V_C is expressed based on z_{ms} and z_{ns} coordinates (Fig. 1) as

$$V_C = \left(\frac{z_{ms}}{h} + \frac{1}{2} \right)^k = \left(\frac{z_{ns} + C}{h} + \frac{1}{2} \right)^k \tag{1}$$

where k is the power law index which takes the value greater or equal to zero and C is the distance of neutral surface from the mid-surface. Material non-homogeneous properties of a functionally graded material plate may be obtained by means of the Voigt rule of mixture (Suresh and Mortensen 1998). Thus, using Eq. (1), the material non-homogeneous properties of FG plate P , as a function of thickness coordinate, become

$$P(z) = P_M + P_{CM} \left(\frac{z_{ns} + C}{h} + \frac{1}{2} \right)^k, \quad P_{CM} = P_C - P_M \tag{2}$$

where P_M and P_C are the corresponding properties of the metal and ceramic, respectively. In the present work, we assume that the elasticity modulus E , and the thermal expansion coefficient α , are described by Eq. (2), while Poisson's ratio ν , is considered to be constant across the thickness. The position of the neutral surface of the FG plate is determined to satisfy the first moment with respect to Young's modulus being zero as follows (Zhang and Zhou 2008)

$$\int_{-h/2}^{h/2} E(z_{ms})(z_{ms} - C) dz_{ms} = 0 \tag{3}$$

Consequently, the position of neutral surface can be obtained as

$$C = \frac{\int_{-h/2}^{h/2} E(z_{ms})z_{ms} dz_{ms}}{\int_{-h/2}^{h/2} E(z_{ms}) dz_{ms}} \tag{4}$$

2.1 The present sinusoidal shear deformation theory for functionally graded plates

Unlike the conventional sinusoidal shear deformation theory (Zenkour and Mashat 2010), the number of unknown functions involved in the present sinusoidal shear deformation theory based on exact neutral surface position is only four. The theory presented is variationally consistent, does not require shear correction factor, and gives rise to the sinusoidal distribution of transverse shear stress across the thickness satisfying shear stress free surface conditions.

2.1.1 Basic assumptions

Assumptions of the present theory are as follows:

(i) The displacements are small in comparison with the plate thickness and, therefore, strains involved are infinitesimal.

(ii) The transverse displacement w includes two components of bending w_b , and shear w_s . These components are functions of coordinates x, y only.

$$w(x, y, z_{ns}) = w_b(x, y) + w_s(x, y) \tag{5}$$

(iii) The transverse normal stress σ_z is negligible in comparison with in-plane stresses σ_x and σ_y .

(iv) The displacements u in x -direction and v in y -direction consist of extension, bending, and shear components.

$$U = u_0 + u_b + u_s, \quad V = v_0 + v_b + v_s \tag{6}$$

The bending components u_b and v_b are assumed to be similar to the displacements given by the classical plate theory. Therefore, the expression for u_b and v_b can be given as

$$u_b = -z_{ns} \frac{\partial w_b}{\partial x}, \quad v_b = -z_{ns} \frac{\partial w_b}{\partial y} \tag{7}$$

The shear components u_s and v_s give rise, in conjunction with w_s , to the parabolic variations of shear strains γ_{xz}, γ_{yz} and hence to shear stresses τ_{xz}, τ_{yz} through the thickness of the plate in such a way that shear stresses τ_{xz}, τ_{yz} are zero at the top and bottom faces of the plate. Consequently, the expression for u_s and v_s can be given as

$$u_s = -f(z_{ns}) \frac{\partial w_s}{\partial x}, \quad v_s = -f(z_{ns}) \frac{\partial w_s}{\partial y} \tag{8}$$

where

$$f(z_{ns}) = \left(z_{ns} + C - \frac{h}{\pi} \sin \frac{\pi(z_{ns} + C)}{h} \right) \tag{9}$$

2.1.2 Kinematics

Based on the assumptions made in the preceding section, the displacement field can be obtained using Eqs. (5)-(9) as

$$u(x, y, z_{ns}) = u_0(x, y) - z_{ns} \frac{\partial w_b}{\partial x} - f(z_{ns}) \frac{\partial w_s}{\partial x} \tag{10a}$$

$$v(x, y, z_{ns}) = v_0(x, y) - z_{ns} \frac{\partial w_b}{\partial y} - f(z_{ns}) \frac{\partial w_s}{\partial y} \tag{10b}$$

$$w(x, y, z_{ns}) = w_b(x, y) + w_s(x, y) \tag{10c}$$

The non-linear von Karman strain–displacement equations are as follows

$$\begin{Bmatrix} \boldsymbol{\varepsilon}_x \\ \boldsymbol{\varepsilon}_y \\ \boldsymbol{\gamma}_{xy} \end{Bmatrix} = \begin{Bmatrix} \boldsymbol{\varepsilon}_x^0 \\ \boldsymbol{\varepsilon}_y^0 \\ \boldsymbol{\gamma}_{xy}^0 \end{Bmatrix} + z_{ns} \begin{Bmatrix} \mathbf{k}_x^b \\ \mathbf{k}_y^b \\ \mathbf{k}_{xy}^b \end{Bmatrix} + f(z_{ns}) \begin{Bmatrix} \mathbf{k}_x^s \\ \mathbf{k}_y^s \\ \mathbf{k}_{xy}^s \end{Bmatrix}, \quad \begin{Bmatrix} \boldsymbol{\gamma}_{yz} \\ \boldsymbol{\gamma}_{xz} \end{Bmatrix} = g(z_{ns}) \begin{Bmatrix} \boldsymbol{\gamma}_{yz}^s \\ \boldsymbol{\gamma}_{xz}^s \end{Bmatrix} \quad (11)$$

where

$$\begin{Bmatrix} \boldsymbol{\varepsilon}_x^0 \\ \boldsymbol{\varepsilon}_y^0 \\ \boldsymbol{\gamma}_{xy}^0 \end{Bmatrix} = \begin{Bmatrix} \frac{\partial u_0}{\partial x} + \frac{1}{2} \left(\frac{\partial w_b}{\partial x} + \frac{\partial w_s}{\partial x} \right)^2 \\ \frac{\partial v_0}{\partial x} + \frac{1}{2} \left(\frac{\partial w_b}{\partial y} + \frac{\partial w_s}{\partial y} \right)^2 \\ \frac{\partial u_0}{\partial y} + \frac{\partial v_0}{\partial x} + \left(\frac{\partial w_b}{\partial x} + \frac{\partial w_s}{\partial x} \right) \left(\frac{\partial w_b}{\partial y} + \frac{\partial w_s}{\partial y} \right) \end{Bmatrix}, \quad \begin{Bmatrix} \mathbf{k}_x^b \\ \mathbf{k}_y^b \\ \mathbf{k}_{xy}^b \end{Bmatrix} = \begin{Bmatrix} -\frac{\partial^2 w_b}{\partial x^2} \\ -\frac{\partial^2 w_b}{\partial y^2} \\ -2\frac{\partial^2 w_b}{\partial x \partial y} \end{Bmatrix}, \quad \begin{Bmatrix} \mathbf{k}_x^s \\ \mathbf{k}_y^s \\ \mathbf{k}_{xy}^s \end{Bmatrix} = \begin{Bmatrix} -\frac{\partial^2 w_s}{\partial x^2} \\ -\frac{\partial^2 w_s}{\partial y^2} \\ -2\frac{\partial^2 w_s}{\partial x \partial y} \end{Bmatrix},$$

$$\begin{Bmatrix} \boldsymbol{\gamma}_{yz}^s \\ \boldsymbol{\gamma}_{xz}^s \end{Bmatrix} = \begin{Bmatrix} \frac{\partial w_s}{\partial y} \\ \frac{\partial w_s}{\partial x} \end{Bmatrix} \quad (12a)$$

and

$$g(z_{ns}) = 1 - \frac{df(z_{ns})}{dz_{ns}} = \cos\left(\frac{\pi(z_{ns} + C)}{h}\right) \quad (12b)$$

2.1.3 Constitutive relations

The plate is subjected to a thermal load $T(x, t, z_{ns})$. The linear constitutive relations are

$$\begin{Bmatrix} \boldsymbol{\sigma}_x \\ \boldsymbol{\sigma}_y \\ \boldsymbol{\tau}_{xy} \end{Bmatrix} = \begin{bmatrix} Q_{11} & Q_{12} & 0 \\ Q_{12} & Q_{22} & 0 \\ 0 & 0 & Q_{66} \end{bmatrix} \begin{Bmatrix} \boldsymbol{\varepsilon}_x - \alpha T \\ \boldsymbol{\varepsilon}_y - \alpha T \\ \boldsymbol{\gamma}_{xy} \end{Bmatrix} \quad \text{and} \quad \begin{Bmatrix} \boldsymbol{\tau}_{yz} \\ \boldsymbol{\tau}_{xz} \end{Bmatrix} = \begin{bmatrix} Q_{44} & 0 \\ 0 & Q_{55} \end{bmatrix} \begin{Bmatrix} \boldsymbol{\gamma}_{yz} \\ \boldsymbol{\gamma}_{xz} \end{Bmatrix} \quad (13)$$

where $(\boldsymbol{\sigma}_x, \boldsymbol{\sigma}_y, \boldsymbol{\tau}_{xy}, \boldsymbol{\tau}_{yz}, \boldsymbol{\tau}_{yx})$ and $(\boldsymbol{\varepsilon}_x, \boldsymbol{\varepsilon}_y, \boldsymbol{\gamma}_{xy}, \boldsymbol{\gamma}_{yz}, \boldsymbol{\gamma}_{yx})$ are the stress and strain components, respectively. Using the material properties defined in Eq. (2), stiffness coefficients, Q_{ij} , can be expressed as

$$Q_{11} = Q_{22} = \frac{E(z_{ns})}{1-\nu^2}, \quad (14a)$$

$$Q_{12} = \frac{\nu E(z_{ns})}{1-\nu^2}, \quad (14b)$$

$$Q_{44} = Q_{55} = Q_{66} = \frac{E(z_{ns})}{2(1+\nu)}, \quad (14c)$$

2.1.4 Stability equations

The total potential energy of the FG plate may be written as

$$U = \frac{1}{2} \iiint [\sigma_x(\epsilon_x - \alpha T) + \sigma_y(\epsilon_y - \alpha T) + \tau_{xy}\gamma_{xy} + \tau_{yz}\gamma_{yz} + \tau_{xz}\gamma_{xz}] dz_{ns} dy dx, \tag{15}$$

The principle of virtual work for the present problem may be expressed as follows

$$\iiint [N_x \delta \epsilon_x^0 + N_y \delta \epsilon_y^0 + N_{xy} \delta \gamma_{xy}^0 + M_x^b \delta k_x^b + M_y^b \delta k_y^b + M_{xy}^b \delta k_{xy}^b + M_x^s \delta k_x^s + M_y^s \delta k_y^s + M_{xy}^s \delta k_{xy}^s + S_{yz}^s \delta \gamma_{yz}^s + S_{xz}^s \delta \gamma_{xz}^s] dx dy = 0 \tag{16}$$

where

$$\begin{Bmatrix} N_x, & N_y, & N_{xy} \\ M_x^b, & M_y^b, & M_{xy}^b \\ M_x^s, & M_y^s, & M_{xy}^s \end{Bmatrix} = \int_{-h/2-C}^{h/2-C} (\sigma_x, \sigma_y, \tau_{xy}) \begin{Bmatrix} 1 \\ z_{ns} \\ f(z_{ns}) \end{Bmatrix} dz_{ns}, \tag{17a}$$

$$(S_{xz}^s, S_{yz}^s) = \int_{-h/2-C}^{h/2-C} (\tau_{xz}, \tau_{yz}) g(z_{ns}) dz_{ns}. \tag{17b}$$

Using Eq. (13) in Eq. (17), the stress resultants of the FG plate can be related to the total strains by

$$\begin{Bmatrix} N \\ M^b \\ M^s \end{Bmatrix} = \begin{bmatrix} A & 0 & B^s \\ 0 & D & D^s \\ B^s & D^s & H^s \end{bmatrix} \begin{Bmatrix} \epsilon \\ k^b \\ k^s \end{Bmatrix} - \begin{Bmatrix} N^T \\ M^{bT} \\ M^{sT} \end{Bmatrix}, \quad S = A^s \gamma, \tag{18}$$

where

$$N = \{N_x, N_y, N_{xy}\}^t, \quad M^b = \{M_x^b, M_y^b, M_{xy}^b\}^t, \quad M^s = \{M_x^s, M_y^s, M_{xy}^s\}^t, \tag{19a}$$

$$N^T = \{N_x^T, N_y^T, 0\}^t, \quad M^{bT} = \{M_x^{bT}, M_y^{bT}, 0\}^t, \quad M^{sT} = \{M_x^{sT}, M_y^{sT}, 0\}^t, \tag{19b}$$

$$\epsilon = \{\epsilon_x^0, \epsilon_y^0, \gamma_{xy}^0\}^t, \quad k^b = \{k_x^b, k_y^b, k_{xy}^b\}^t, \quad k^s = \{k_x^s, k_y^s, k_{xy}^s\}^t, \tag{19c}$$

$$A = \begin{bmatrix} A_{11} & A_{12} & 0 \\ A_{12} & A_{22} & 0 \\ 0 & 0 & A_{66} \end{bmatrix}, \quad D = \begin{bmatrix} D_{11} & D_{12} & 0 \\ D_{12} & D_{22} & 0 \\ 0 & 0 & D_{66} \end{bmatrix}, \tag{19d}$$

$$B^s = \begin{bmatrix} B_{11}^s & B_{12}^s & 0 \\ B_{12}^s & B_{22}^s & 0 \\ 0 & 0 & B_{66}^s \end{bmatrix}, \quad D^s = \begin{bmatrix} D_{11}^s & D_{12}^s & 0 \\ D_{12}^s & D_{22}^s & 0 \\ 0 & 0 & D_{66}^s \end{bmatrix}, \quad H^s = \begin{bmatrix} H_{11}^s & H_{12}^s & 0 \\ H_{12}^s & H_{22}^s & 0 \\ 0 & 0 & H_{66}^s \end{bmatrix}, \tag{19e}$$

$$S = \{S_{yz}^s, S_{xz}^s\}^t, \quad \gamma = \{\gamma_{yz}, \gamma_{xz}\}^t, \quad A^s = \begin{bmatrix} A_{44}^s & 0 \\ 0 & A_{55}^s \end{bmatrix}, \tag{19f}$$

where A_{ij} , D_{ij} , etc., are the plate stiffness, defined by

$$\begin{Bmatrix} A_{11} & D_{11} & B_{11}^s & D_{11}^s & H_{11}^s \\ A_{12} & D_{12} & B_{12}^s & D_{12}^s & H_{12}^s \\ A_{66} & D_{66} & B_{66}^s & D_{66}^s & H_{66}^s \end{Bmatrix} = \int_{-\frac{h-c}{2}}^{\frac{h-c}{2}} Q_{11} \left(1, z^2, f(z_{ns}), z_{ns} f(z_{ns}), f^2(z_{ns}) \right) \begin{Bmatrix} 1 \\ \nu \\ \frac{1-\nu}{2} \end{Bmatrix} dz_{ns}, \tag{20a}$$

and

$$(A_{22}, D_{22}, B_{22}^s, D_{22}^s, H_{22}^s) = (A_{11}, D_{11}, B_{11}^s, D_{11}^s, H_{11}^s), \tag{20b}$$

$$A_{44}^s = A_{55}^s = \int_{-\frac{h-c}{2}}^{\frac{h-c}{2}} \frac{E(z_{ns})}{2(1+\nu)} [g(z_{ns})]^2 dz_{ns}, \tag{20c}$$

The stress and moment resultants, $N_x^T = N_y^T$, $M_x^{bT} = M_y^{bT}$, and $M_x^{sT} = M_y^{sT}$ due to thermal loading are defined by

$$\begin{Bmatrix} N_x^T \\ M_x^{bT} \\ M_x^{sT} \end{Bmatrix} = \int_{-\frac{h-c}{2}}^{\frac{h-c}{2}} \frac{E(z_{ns})}{1-\nu} \alpha(z_{ns}) T \begin{Bmatrix} 1 \\ z \\ f(z_{ns}) \end{Bmatrix} dz_{ns}, \tag{21}$$

The stability equations of the plate may be derived by the adjacent equilibrium criterion. Assume that the equilibrium state of the FG plate under thermal loads is defined in terms of the displacement components $(u_0^0, v_0^0, w_b^0, w_s^0)$. The displacement components of a neighboring stable state differ by $(u_0^1, v_0^1, w_b^1, w_s^1)$ with respect to the equilibrium position. Thus, the total displacements of a neighboring state are

$$u_0 = u_0^0 + u_0^1, \quad v_0 = v_0^0 + v_0^1, \quad w_b = w_b^0 + w_b^1, \quad w_s = w_s^0 + w_s^1 \tag{22}$$

where the superscript 1 refers to the state of stability and the superscript 0 refers to the state of equilibrium conditions.

Substituting Eqs. (11) and (22) into Eq. (16) and integrating by parts and then equating the coefficients of δu_0^1 , δv_0^1 , δw_b^1 and δw_s^1 to zero, separately, the governing stability equations are obtained for the shear deformation plate theories as

$$\begin{aligned} \frac{\partial N_x^1}{\partial x} + \frac{\partial N_{xy}^1}{\partial y} &= 0 \\ \frac{\partial N_{xy}^1}{\partial x} + \frac{\partial N_y^1}{\partial y} &= 0 \\ \frac{\partial^2 M_x^{b1}}{\partial x^2} + 2 \frac{\partial^2 M_{xy}^{b1}}{\partial x \partial y} + \frac{\partial^2 M_y^{b1}}{\partial y^2} + \bar{N} &= 0 \\ \frac{\partial^2 M_x^{s1}}{\partial x^2} + 2 \frac{\partial^2 M_{xy}^{s1}}{\partial x \partial y} + \frac{\partial^2 M_y^{s1}}{\partial y^2} + \frac{\partial S_{xz}^{s1}}{\partial x} + \frac{\partial S_{yz}^{s1}}{\partial y} + \bar{N} &= 0 \end{aligned} \tag{23}$$

with

$$\bar{N} = \left[N_x^0 \frac{\partial^2(w_b^1 + w_s^1)}{\partial x^2} + N_y^0 \frac{\partial^2(w_b^1 + w_s^1)}{\partial y^2} \right] \tag{24}$$

where the terms N_x^0 and N_y^0 are the pre-buckling force resultants obtained as

$$N_x^0 = N_y^0 = - \int_{-\frac{h}{2}-c}^{\frac{h}{2}-c} \frac{\alpha(z_{ms})E(z_{ms})T}{1-\nu} dz_{ms} \tag{25}$$

The stability equations in terms of the displacement components may be obtained by substituting Eq. (18) into Eq. (23). Resulting equations are four stability equations based on the present refined shear deformation theory for FG plates in contact with two parameters elastic foundation

$$A_{11} \frac{\partial^2 u_0^1}{\partial x^2} + A_{66} \frac{\partial^2 u_0^1}{\partial y^2} + (A_{12} + A_{66}) \frac{\partial^2 v_0^1}{\partial x \partial y} - B_{11}^s \frac{\partial^3 w_s^1}{\partial x^3} - (B_{12}^s + 2B_{66}^s) \frac{\partial^3 w_s^1}{\partial x \partial y^2} = 0 \tag{26a}$$

$$(A_{12} + A_{66}) \frac{\partial^2 u_0^1}{\partial x \partial y} + A_{66} \frac{\partial^2 v_0^1}{\partial x^2} + A_{22} \frac{\partial^2 v_0^1}{\partial y^2} - B_{22}^s \frac{\partial^3 w_s^1}{\partial y^3} - (B_{12}^s + 2B_{66}^s) \frac{\partial^3 w_s^1}{\partial x^2 \partial y} = 0 \tag{26b}$$

$$-D_{11} \frac{\partial^4 w_b^1}{\partial x^4} - 2(D_{12} + 2D_{66}) \frac{\partial^4 w_b^1}{\partial x^2 \partial y^2} - D_{22} \frac{\partial^4 w_b^1}{\partial y^4} - D_{11}^s \frac{\partial^4 w_s^1}{\partial x^4} - 2(D_{12}^s + 2D_{66}^s) \frac{\partial^4 w_s^1}{\partial x^2 \partial y^2} - D_{22}^s \frac{\partial^4 w_s^1}{\partial y^4} + \bar{N}^1 = 0 \tag{26c}$$

$$B_{11}^s \frac{\partial^3 u_0^1}{\partial x^3} + (B_{12}^s + 2B_{66}^s) \frac{\partial^3 u_0^1}{\partial x \partial y^2} + (B_{12}^s + 2B_{66}^s) \frac{\partial^3 v_0^1}{\partial x^2 \partial y} + B_{22}^s \frac{\partial^3 v_0^1}{\partial y^3} - D_{11}^s \frac{\partial^4 w_b^1}{\partial x^4} - 2(D_{12}^s + 2D_{66}^s) \frac{\partial^4 w_b^1}{\partial x^2 \partial y^2} - D_{22}^s \frac{\partial^4 w_b^1}{\partial y^4} - H_{11}^s \frac{\partial^4 w_s^1}{\partial x^4} - 2(H_{12}^s + 2H_{66}^s) \frac{\partial^4 w_s^1}{\partial x^2 \partial y^2} - H_{22}^s \frac{\partial^4 w_s^1}{\partial y^4} + A_{55}^s \frac{\partial^2 w_s^1}{\partial x^2} + A_{44}^s \frac{\partial^2 w_s^1}{\partial y^2} + \bar{N}^1 = 0 \tag{26d}$$

4. Trigonometric solution to thermal buckling

Rectangular plates are generally classified in accordance with the type of support used. We are here concerned with the exact solution of Eq. (26) for a simply supported FG plate. The following boundary conditions are imposed for the present efficient sinusoidal shear deformation theory at the side edges

$$v_0^1 = w_b^1 = w_s^1 = \frac{\partial w_s^1}{\partial y} = N_x^1 = M_x^{b1} = M_x^{s1} = 0 \text{ at } x=0, a, \tag{27a}$$

$$u_0^1 = w_b^1 = w_s^1 = \frac{\partial w_s^1}{\partial x} = N_y^1 = M_y^{b1} = M_y^{s1} = 0 \text{ at } y=0, b. \tag{27b}$$

The following approximate solution is seen to satisfy both the differential equation and the

boundary conditions

$$\begin{Bmatrix} u_0^1 \\ v_0^1 \\ w_b^1 \\ w_s^1 \end{Bmatrix} = \sum_{m=1}^{\infty} \sum_{n=1}^{\infty} \begin{Bmatrix} U_{mn}^1 \cos(\lambda x) \sin(\mu y) \\ V_{mn}^1 \sin(\lambda x) \cos(\mu y) \\ W_{bmn}^1 \sin(\lambda x) \sin(\mu y) \\ W_{smn}^1 \sin(\lambda x) \sin(\mu y) \end{Bmatrix} \quad (28)$$

where U_{mn}^1 , V_{mn}^1 , W_{bmn}^1 , and W_{smn}^1 are arbitrary parameters to be determined and $\lambda = m\pi/a$ and $\mu = n\pi/b$. Substituting Eq. (28) into Eq. (26), one obtains

$$[\mathbf{K}]\{\Delta\} = 0, \quad (29)$$

where $\{\Delta\}$ denotes the column

$$\{\Delta\} = \{U_{mn}^1, V_{mn}^1, W_{bmn}^1, W_{smn}^1\}^t \quad (30)$$

and $[\mathbf{K}]$ is the symmetric matrix given by

$$[\mathbf{K}] = \begin{bmatrix} a_{11} & a_{12} & a_{13} & a_{14} \\ a_{12} & a_{22} & a_{23} & a_{24} \\ a_{13} & a_{23} & a_{33} & a_{34} \\ a_{14} & a_{24} & a_{34} & a_{44} \end{bmatrix}, \quad (31)$$

in which

$$\begin{aligned} a_{11} &= -(A_{11}\lambda^2 + A_{66}\mu^2) \\ a_{12} &= -\lambda\mu(A_{12} + A_{66}) \\ a_{13} &= 0 \\ a_{14} &= \lambda[B_{11}^s\lambda^2 + (B_{12}^s + 2B_{66}^s)\mu^2] \\ a_{22} &= -(A_{66}\lambda^2 + A_{22}\mu^2) \\ a_{23} &= 0 \\ a_{24} &= \mu[(B_{12}^s + 2B_{66}^s)\lambda^2 + B_{22}^s\mu^2] \\ a_{33} &= -(D_{11}\lambda^4 + 2(D_{12} + 2D_{66})\lambda^2\mu^2 + D_{22}\mu^4 + N_x^0\lambda^2 + N_y^0\mu^2) \\ a_{34} &= -(D_{11}^s\lambda^4 + 2(D_{12}^s + 2D_{66}^s)\lambda^2\mu^2 + D_{22}^s\mu^4 + N_x^0\lambda^2 + N_y^0\mu^2) \\ a_{44} &= -(H_{11}^s\lambda^4 + 2(H_{12}^s + 2H_{66}^s)\lambda^2\mu^2 + H_{22}^s\mu^4 + A_{55}^s\lambda^2 + A_{44}^s\mu^2 + N_x^0\lambda^2 + N_y^0\mu^2) \end{aligned} \quad (32)$$

By applying the static condensation approach to eliminate the coefficients associated with the in-plane displacements, Eq. (29) can be rewritten as

$$\begin{bmatrix} [\mathbf{K}^{11}] \\ [\mathbf{K}^{12}]^T \end{bmatrix} \begin{bmatrix} \mathbf{K}^{12} \\ \mathbf{K}^{22} \end{bmatrix} \begin{Bmatrix} \Delta^1 \\ \Delta^2 \end{Bmatrix} = \begin{Bmatrix} 0 \\ 0 \end{Bmatrix} \quad (33)$$

where

$$[\mathbf{K}^{11}] = \begin{bmatrix} \mathbf{a}_{11} & \mathbf{a}_{12} \\ \mathbf{a}_{12} & \mathbf{a}_{22} \end{bmatrix}, [\mathbf{K}^{12}] = \begin{bmatrix} 0 & \mathbf{a}_{14} \\ 0 & \mathbf{a}_{24} \end{bmatrix}, [\mathbf{K}^{22}] = \begin{bmatrix} \mathbf{a}_{33} & \mathbf{a}_{34} \\ \mathbf{a}_{34} & \mathbf{a}_{44} \end{bmatrix} \quad (34a)$$

$$\Delta^1 = \begin{Bmatrix} \mathbf{U}_{mn}^1 \\ \mathbf{V}_{mn}^1 \end{Bmatrix}, \Delta^2 = \begin{Bmatrix} \mathbf{W}_{bmn}^1 \\ \mathbf{W}_{smn}^1 \end{Bmatrix} \quad (34b)$$

Eq. (33) represents a pair of two matrix equations

$$[\mathbf{K}^{11}]\Delta^1 + [\mathbf{K}^{12}]\Delta^2 = 0 \quad (35a)$$

$$[\mathbf{K}^{12}]^T \Delta^1 + [\mathbf{K}^{22}]\Delta^2 = 0 \quad (35b)$$

Solving Eq. (35a) for Δ^1 and then substituting the result into Eq. (35b), the following equation is obtained

$$[\bar{\mathbf{K}}^{22}]\Delta^2 = 0 \quad (36)$$

where

$$[\bar{\mathbf{K}}^{22}] = [\mathbf{K}^{22}] - [\mathbf{K}^{12}]^T [\mathbf{K}^{11}]^{-1} [\mathbf{K}^{12}] = \begin{bmatrix} \bar{\mathbf{a}}_{33} & \bar{\mathbf{a}}_{34} \\ \bar{\mathbf{a}}_{43} & \bar{\mathbf{b}}_{44} \end{bmatrix} \quad (37a)$$

and

$$\begin{aligned} \bar{\mathbf{a}}_{33} &= \mathbf{a}_{33}, \quad \bar{\mathbf{a}}_{34} = \mathbf{a}_{34} \\ \bar{\mathbf{a}}_{43} &= \mathbf{a}_{34}, \quad \bar{\mathbf{b}}_{44} = \mathbf{a}_{44} - \mathbf{a}_{14} \frac{\mathbf{b}_1}{\mathbf{b}_0} - \mathbf{a}_{24} \frac{\mathbf{b}_2}{\mathbf{b}_0} \\ \mathbf{b}_0 &= \mathbf{a}_{11}\mathbf{a}_{22} - \mathbf{a}_{12}^2, \quad \mathbf{b}_1 = \mathbf{a}_{14}\mathbf{a}_{22} - \mathbf{a}_{12}\mathbf{a}_{24}, \quad \mathbf{b}_2 = \mathbf{a}_{11}\mathbf{a}_{24} - \mathbf{a}_{12}\mathbf{a}_{14} \end{aligned} \quad (37b)$$

For nontrivial solution, the determinant of the coefficient matrix in Eq. (36) must be zero. This gives the following expression for the thermal buckling load

$$N_x^0 = N_y^0 = \frac{1}{\lambda^2 + \mu^2} \frac{\mathbf{a}_{33}\mathbf{b}_{44} - \mathbf{a}_{34}^2}{\mathbf{a}_{33} + \mathbf{a}_{44} - 2\mathbf{a}_{34}} \quad (38)$$

4.1 Buckling of FG plates under uniform temperature rise

The plate initial temperature is assumed to be T_i . The temperature is uniformly raised to a final value T_f in which the plate buckles. The temperature change is $\Delta T = T_f - T_i$. Using this distribution of temperature, the critical buckling temperature change ΔT_{cr} becomes b5 using Eqs. (24) and (38)

$$\Delta T_{cr} = \frac{1}{\beta_1(\lambda^2 + \mu^2)} \frac{\mathbf{a}_{33}\mathbf{b}_{44} - \mathbf{a}_{34}^2}{\mathbf{a}_{33} + \mathbf{a}_{44} - 2\mathbf{a}_{34}} \quad (39a)$$

where

$$\bar{\beta}_1 = - \int_{-h/2-C}^{h/2-C} \frac{\alpha(z_{ns})E(z_{ns})}{1-\nu} dz_{ns}. \quad (39b)$$

4.2 Buckling of FG plates under linear temperature rise

For FG plates, the temperature change is not uniform. The temperature is assumed to be varied linearly through the thickness as follows

$$T(z_{ns}) = \Delta T \left(\frac{z_{ns} + C}{h} + \frac{1}{2} \right) + T_M, \quad (40)$$

where the buckling temperature difference $\Delta T = T_C - T_M$ and T_C and T_M are the temperature of the top surface which is ceramic-rich and the bottom surface which is metal-rich, respectively.

Similar to the previous loading case, the critical buckling temperature difference ΔT_{cr} can be determined as

$$\Delta T_{cr} = \frac{a_{33}b_{44} - a_{34}^2 + T_M \bar{\beta}_1 (\lambda^2 + \mu^2) (a_{33} + a_{44} - 2a_{34})}{\bar{\beta}_2 (\lambda^2 + \mu^2) (a_{33} + a_{44} - 2a_{34})} \quad (41a)$$

where

$$\bar{\beta}_2 = - \int_{-h/2-C}^{h/2-C} \frac{\alpha(z_{ns})E(z_{ns})}{1-\nu} \left(\frac{z_{ns} + C}{h} + \frac{1}{2} \right) dz_{ns} \quad (41b)$$

4.3 Buckling of FG plates subjected to graded temperature change across the thickness

We assume that the temperature of the top surface is T_M and the temperature varies from T_M , according to the power law variation through-the-thickness, to the bottom surface temperature T_M in which the plate buckles. In this case, the temperature through-the-thickness is given by

$$T(z_{ns}) = \Delta T \left(\frac{z_{ns} + C}{h} + \frac{1}{2} \right)^\gamma + T_M, \quad (42)$$

where the buckling temperature difference $\Delta T = T_C - T_M$ and γ is the temperature exponent ($0 < \gamma < \infty$). Note that the value of γ equal to unity represents a linear temperature change across the thickness. While the value of γ excluding unity represents a non-linear temperature change through-the-thickness.

Similar to the previous loading case, the critical buckling temperature change ΔT_{cr} becomes by using Eqs. (25) and (38)

$$\Delta T_{cr} = \frac{a_{33}b_{44} - a_{34}^2 + T_M \bar{\beta}_1 (\lambda^2 + \mu^2) (a_{33} + a_{44} - 2a_{34})}{\bar{\beta}_3 (\lambda^2 + \mu^2) (a_{33} + a_{44} - 2a_{34})} \quad (34a)$$

where

$$\bar{\beta}_3 = - \int_{-h/2-C}^{h/2-C} \frac{\alpha(z_{ns})E(z_{ns})}{1-\nu} \left(\frac{z_{ns} + C}{h} + \frac{1}{2} \right)^{\gamma} dz_{ns} \tag{34b}$$

5. Results and discussion

In order to obtain the numerical results, an Al/Al₂O₃ functionally graded plate composed of Aluminum and Alumina is considered. The Young modulus and coefficient of thermal expansion for Aluminum are $E_M=70\text{GPa}$, $\alpha_M=23.10^{-6}/^{\circ}\text{C}$ and for Alumina are $E_C=380\text{GPa}$, $\alpha_C=7.4^{-6}/^{\circ}\text{C}$, respectively. The Poisson’s ratio of the plate is assumed to be constant through the thickness and equal to 0.3.

For the linear and non-linear temperature rises through the thickness, the temperature rises 5 °C in the metal-rich surface of the plate (i.e., $T_m=5^{\circ}\text{C}$).

5.1 Comparative studies

In order to demonstrate the accuracy of the present closed-form exact solution, some comparisons of the present results with those available in the literature has been carried out. In Tables 1 and 2, the plate under uniform temperature rise is considered and the critical buckling temperature change obtained from present efficient sinusoidal shear deformation theory have been compared with those reported by Javaheri and Eslami (2002b) based on both higher plate theory (HPT) and the classical plate theory (CPT), and Zenkour and Mashat (2010) based on sinusoidal plate theory (SPT). From the results presented in Tables 1 and 2, it is observed that results have a good agreement.

Table 1 Critical buckling temperature of FG plate under uniform temperature rise for different values of power law index k and aspect ratio a/b with $a/h=100$

k	Theory	$a/b = 1$	$a/b = 2$	$a/b = 3$	$a/b = 4$	$a/b = 5$
0	Present	17.08	42.68	85.25	144.64	220.67
	Javaheri and Eslami (2002b): HPT	17.08	42.68	85.25	144.64	220.66
	Zenkour and Mashat (2010): SPT	17.08	42.68	85.25	144.65	220.67
	Javaheri and Eslami (2002b): CPT	17.09	42.74	85.49	145.34	222.28
	Present	7.93	19.83	39.62	67.25	102.63
1	Javaheri and Eslami (2002b): HPT	7.94	19.83	39.62	67.25	102.63
	Zenkour and Mashat (2010): SPT	7.94	19.83	39.62	67.25	102.63
	Javaheri and Eslami (2002b): CPT	7.94	19.85	39.71	67.52	103.26
	Present	7.26	18.13	36.20	61.39	93.60
5	Javaheri and Eslami (2002b): HPT	7.26	18.13	36.20	61.39	93.60
	Zenkour and Mashat (2010): SPT	7.26	18.13	36.20	61.39	93.60
	Javaheri and Eslami (2002b): CPT	7.26	18.16	36.32	61.75	94.45
	Present	7.46	18.63	37.20	63.06	96.11
10	Javaheri and Eslami (2002b): HPT	7.46	18.63	37.20	63.06	96.12
	Zenkour and Mashat (2010): SPT	7.46	18.63	37.20	63.06	96.11
	Javaheri and Eslami (2002b): CPT	7.46	18.67	37.34	63.48	97.10

Table 2 Critical buckling temperature of square FG plate under uniform temperature rise for different values of power law index k and side-to-thickness ratio a/h

k	Theory	$a/h=10$	$a/h=20$	$a/h=40$	$a/h=60$	$a/h=80$	$a/h=100$
0	Present	1618.82	421.54	106.49	47.42	26.69	17.08
	Javaheri and Eslami (2002b): HPT	1617.48	421.52	106.49	47.42	26.69	17.08
	Javaheri and Eslami (2002b): CPT	1709.91	427.47	106.87	47.49	26.71	17.09
1	Present	758.47	196.26	49.50	22.03	12.40	7.94
	Javaheri and Eslami (2002b): HPT	757.89	196.26	49.50	22.03	12.40	7.94
	Javaheri and Eslami (2002b): CPT	794.37	198.59	49.64	22.06	12.41	7.94
5	Present	678.94	178.50	45.21	20.14	11.34	7.26
	Javaheri and Eslami (2002b): HPT	678.92	178.53	45.21	20.14	11.34	7.26
	Javaheri and Eslami (2002b): CPT	726.57	181.64	45.41	20.18	11.35	7.26
10	Present	692.54	183.13	46.45	20.70	11.65	7.46
	Javaheri and Eslami (2002b): HPT	692.52	183.14	46.45	20.70	11.65	7.46
	Javaheri and Eslami (2002b): CPT	746.92	186.73	46.68	20.74	11.67	7.46

Table 3 Critical buckling temperature of FG plate under linear temperature rise for different values of power law index k and aspect ratio a/b with $a/h=100$

k	Theory	$a/b=1$	$a/b=2$	$a/b=3$	$a/b=4$	$a/b=5$
0	Present	24.17	75.37	160.51	279.30	431.34
	Javaheri and Eslami (2002b): HPT	24.17	75.37	160.50	279.29	431.33
	Zenkour and Mashat (2010): SPT	24.17	75.37	160.51	279.30	431.34
	Javaheri and Eslami (2002b): CPT	24.19	75.49	160.99	280.68	434.57
1	Present	5.51	27.82	64.93	116.74	183.11
	Javaheri and Eslami (2002b): HPT	5.51	27.82	64.93	116.74	183.11
	Zenkour and Mashat (2010): SPT	5.51	27.82	64.93	116.74	183.11
	Javaheri and Eslami (2002b): CPT	5.52	27.86	65.11	117.25	184.30
5	Present	3.89	22.60	53.70	97.07	152.51
	Javaheri and Eslami (2002b): HPT	3.89	22.60	53.71	97.07	152.51
	Zenkour and Mashat (2010): SPT	3.89	22.60	53.70	97.06	152.50
	Javaheri and Eslami (2002b): CPT	3.89	22.65	53.92	97.69	153.97
10	Present	4.36	24.16	57.06	102.89	161.46
	Javaheri and Eslami (2002b): HPT	4.36	24.16	57.06	102.90	161.47
	Zenkour and Mashat (2010): SPT	4.36	24.16	57.06	102.89	161.46
	Javaheri and Eslami (2002b): CPT	4.37	24.23	57.32	103.64	163.20

Another comparative study for evaluation of critical buckling temperatures between the presented theory based on exact neutral surface position and analytical solution developed by Javaheri and Eslami (2002b) based on HPT, and by Zenkour and Mashat (2010) based on SPT, is performed in Tables 3 and 4. The plate here is subjected to a linear temperature rise across the thickness. From the results presented in Tables 3 and 4, it is observed that results have a good agreement.

Furthermore, in Tables 5 and 6, an interesting comparison study of the present theory with the analytical solution developed by Javaheri and Eslami (2002b) based on HPT, and by Zenkour and

Table 4 Critical buckling temperature of square FG plate under linear temperature rise for different values of power law index k and side-to-thickness ratio a/h

k	Theory	$a/h=10$	$a/h=20$	$a/h=40$	$a/h=60$	$a/h=80$	$a/h=100$
0	Present	3227.36	833.07	202.98	84.84	43.38	24.17
	Javaheri and Eslami (2002b): HPT	3224.96	833.03	202.98	84.84	43.38	24.17
	Javaheri and Eslami (2002b): CPT	3409.82	844.95	203.73	84.99	43.43	24.19
1	Present	1412.96	358.71	83.46	31.95	13.88	5.51
	Javaheri and Eslami (2002b): HPT	1412.02	358.69	83.46	31.95	13.88	5.51
	Javaheri and Eslami (2002b): CPT	1480.45	363.07	83.73	32.00	13.90	5.52
5	Present	1160.68	298.70	69.21	26.06	10.91	3.89
	Javaheri and Eslami (2002b): HPT	1160.02	298.69	69.21	26.06	10.91	3.89
	Javaheri and Eslami (2002b): CPT	1242.03	304.05	69.55	26.13	10.93	3.89
10	Present	1218.63	315.68	73.46	27.82	11.79	4.36
	Javaheri and Eslami (2002b): HPT	1218.32	315.67	73.46	27.82	11.79	4.36
	Javaheri and Eslami (2002b): CPT	1314.74	322.04	73.86	27.90	11.82	4.37

Table 5 Critical buckling temperature of FG plate under non-linear temperature rise for different values of power law index k and aspect ratio a/b , and temperature exponent γ with $a/h=10$

k	Theory	$a/b=1$			$a/b=2$			$a/b=3$		
		$\gamma=2$	$\gamma=5$	$\gamma=10$	$\gamma=2$	$\gamma=5$	$\gamma=10$	$\gamma=2$	$\gamma=5$	$\gamma=10$
0	Present	4.84	9.68	17.75	11.22	22.45	41.17	20.01	40.03	73.39
	Theory 1	4.84	9.68	17.75	11.22	22.45	41.16	20.00	40.01	73.35
	Theory 2	4.84	9.68	17.75	11.22	22.45	41.17	20.01	40.03	73.39
	Theory 3	5.11	10.22	18.75	12.80	25.61	46.96	25.63	51.26	93.99
1	Present	2.10	4.31	8.19	4.95	10.14	19.25	8.97	18.38	34.87
	Theory 1	2.1066	4.31	8.19	4.95	10.14	19.24	8.96	18.38	34.86
	Theory 2	2.1068	4.31	8.19	9.95	10.14	19.25	8.97	18.38	34.87
	Theory 3	2.20	4.52	8.58	5.53	11.35	21.53	11.09	22.73	43.12
5	Present	1.59	2.84	4.99	3.64	6.51	11.43	6.36	11.36	19.93
	Theory 1	1.59	2.85	5.00	3.65	6.52	11.44	6.37	11.38	19.97
	Theory 2	1.59	2.84	4.99	3.64	6.51	11.43	6.36	11.36	19.93
	Theory 3	1.70	3.04	5.35	4.28	7.65	13.43	8.58	15.33	26.90
10	Present	1.67	2.88	4.77	3.79	6.53	10.80	6.53	11.24	18.60
	Theory 1	1.67	2.88	4.77	3.79	6.53	10.80	6.54	11.25	18.61
	Theory 2	1.67	2.88	4.77	3.79	6.53	10.80	6.53	11.24	18.60
	Theory 3	1.80	3.11	5.14	4.54	7.81	12.92	9.09	15.64	25.88

Theory 1: Zenkour and Mashat (2010) based on HPT

Theory 2: Zenkour and Mashat (2010) based on SPT

Theory 3: Zenkour and Mashat (2010) based on CPT

Mashat (2010) based on SPT. Tables 5 and 6 exhibit the critical temperature difference $t_{cr}=10^{-3}T_{cr}$ for different values of the aspect ratio a/b , the temperature exponent γ and the power law index k under non-linear temperature loads at $a/h=10$ and 5, respectively. These tables indicate that our presented results are accurate.

Table 6 Critical buckling temperature of FG plate under non-linear temperature rise for different values of power law index k and aspect ratio a/b , and temperature exponent γ with $a/h=5$

k	Theory	$a/b=1$			$a/b=2$			$a/b=3$		
		$\gamma=2$	$\gamma=5$	$\gamma=10$	$\gamma=2$	$\gamma=5$	$\gamma=10$	$\gamma=2$	$\gamma=5$	$\gamma=10$
0	Present	16.74	33.48	61.38	32.89	65.79	120.62	48.65	97.30	178.39
	Theory 1	16.73	33.47	61.36	32.86	65.72	120.49	48.53	97.07	177.97
	Theory 2	16.74	33.48	61.38	32.89	65.79	120.62	48.65	97.30	178.39
	Theory 3	20.50	41.00	75.18	51.28	102.56	188.03	102.57	205.15	376.12
1	Present	7.45	17.28	28.99	15.09	30.93	58.68	22.97	47.08	89.30
	Theory 1	7.45	15.28	28.98	15.08	30.90	58.62	22.92	46.98	89.11
	Theory 2	7.45	15.28	28.99	15.09	30.93	58.68	22.97	47.08	89.30
	Theory 3	8.87	18.18	34.48	22.19	45.49	86.30	44.41	91.02	172.65
5	Present	5.36	9.57	16.81	10.14	18.10	31.77	14.49	25.87	45.40
	Theory 1	5.37	9.59	16.83	10.16	18.15	31.85	14.52	25.93	45.51
	Theory 2	5.36	9.57	16.81	10.14	18.10	31.77	14.49	25.87	45.40
	Theory 3	6.86	12.26	21.52	17.18	30.68	53.85	34.39	61.39	107.75
10	Present	5.53	9.52	15.75	10.23	17.61	29.13	14.35	24.69	40.85
	Theory 1	5.54	9.53	15.76	10.24	17.62	29.15	14.34	24.68	40.82
	Theory 2	5.53	9.52	15.75	10.23	17.61	29.13	14.35	24.69	40.85
	Theory 3	7.27	12.51	20.70	18.20	31.31	51.80	36.41	62.65	103.64

Theory 1: Zenkour and Mashat (2010) based on HPT

Theory 2: Zenkour and Mashat (2010) based on SPT

Theory 3: Zenkour and Mashat (2010) based on CPT

Finally, the present comparative studies show that the results obtained from the proposed method agree well with existing analytical results in the literature which validate the reliability and accuracy of the present analytical approach. It should be noted that the proposed sinusoidal shear deformation theory based on exact neutral surface position involves four unknowns as against five in case of conventional SPT (Zenkour and Mashat 2010) and HPT (Javaheri and Eslami 2002b).

5.2 Parametric investigations

In this section, to examine the effects of different parameters of plate and the type of thermal loads on the critical buckling load parameter a FG plate, the comprehensive results are illustrated in Figs. 2 to 5.

The variation of critical buckling temperatures of Al/Al₂O₃ FG plates with simply supported edges and subjected to uniform, linear and nonlinear temperature rises are shown in Figs. 2 and 3 with respect to the power law index for several values of the side-to-thickness ratio a/h and aspect ratio a/b , respectively. For the present material properties, the critical buckling temperatures decrease rapidly within the range of $k=0$ (ceramic rich) to $k=5$. As the power law index k becomes larger, all the critical buckling temperatures approach slowly to the values for $k=\infty$ (metallic rich).

It can be also seen from these figures that, regardless of the loading type and the power-law index k , the critical buckling temperature difference t_{cr} decreases as the side-to-thickness ratio a/h increases and it is reduced with the decrease of the aspect ratio a/b . The critical buckling

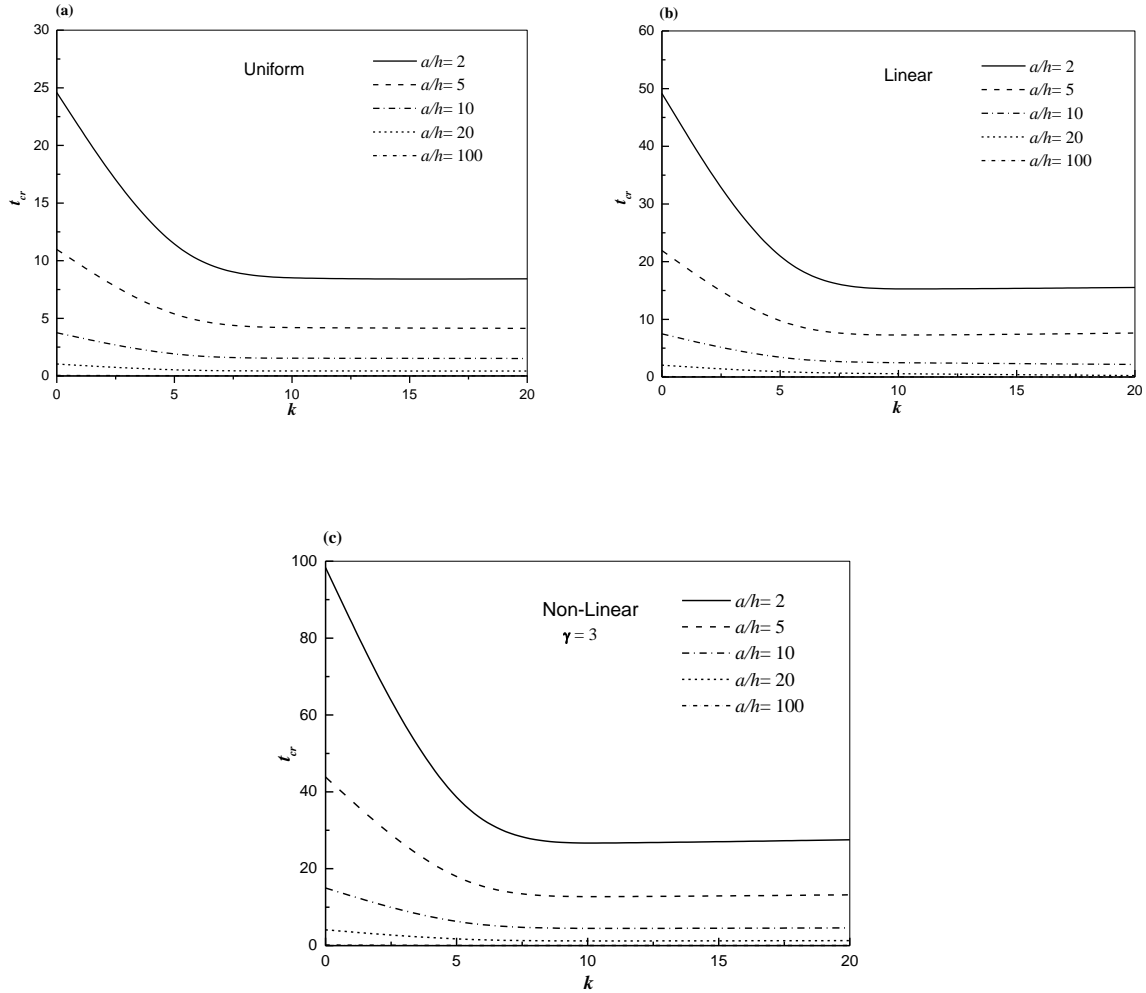


Fig. 2 Critical buckling temperature difference t_{cr} due to uniform, linear and non-linear temperature rise across the thickness of FG plate ($a/b=2$) versus the power law index k for different values of the side-to-thickness ratio a/h

temperature for the ceramic plate is higher than that for the FG plate. This is because the ceramic plate is stronger than the other. The differences between the loading types decrease with the increase of a/h because the plate becomes thin.

The critical buckling temperature change t_{cr} versus the side-to-thickness ratio a/h and the aspect ratio a/b of FG plates under various thermal loading types is exhibited in Figs. 4 and 5. It can be seen from these figures that, regardless of the loading type, the critical buckling temperature difference t_{cr} decreases as the side-to-thickness ratio a/h increases and it is reduced with the decrease of the aspect ratio a/b . It is also observed that the t_{cr} increases with the increase of the non-linearity parameter γ .

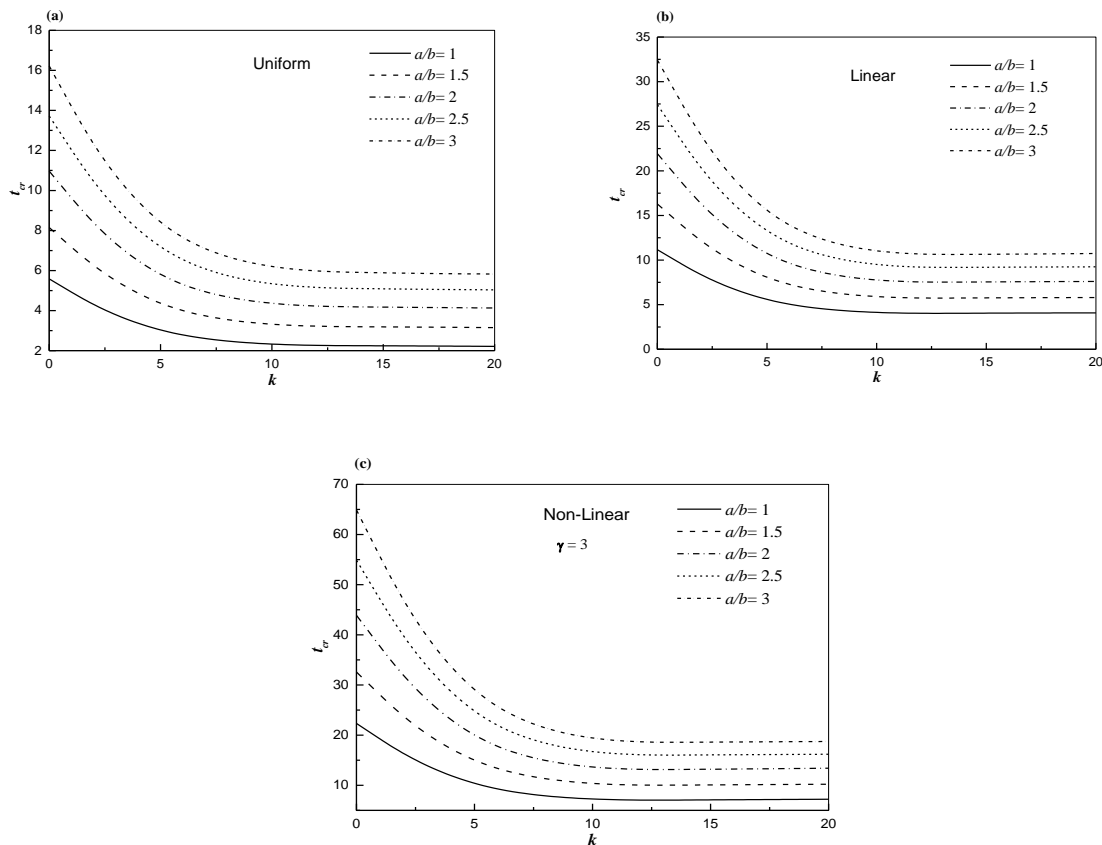


Fig. 3 Critical buckling temperature difference t_{cr} due to uniform, linear and non-linear temperature rise across the thickness of FG plate ($a/h=5$) versus the power law index k for different values of the aspect ratio a/b

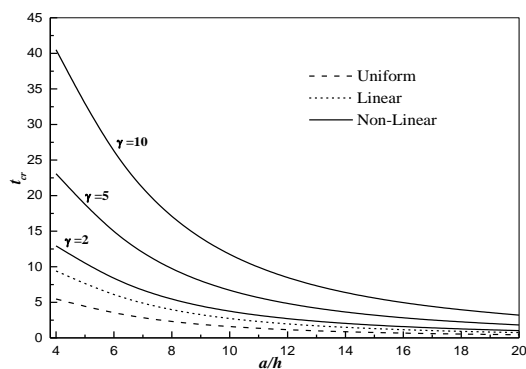


Fig. 4 Critical buckling temperature difference t_{cr} due to uniform, linear and non-linear temperature rise across the thickness versus the side-to-thickness ratio a/h and for different values of the non-linearity parameter γ ($k=5$ and $a/b=2$)

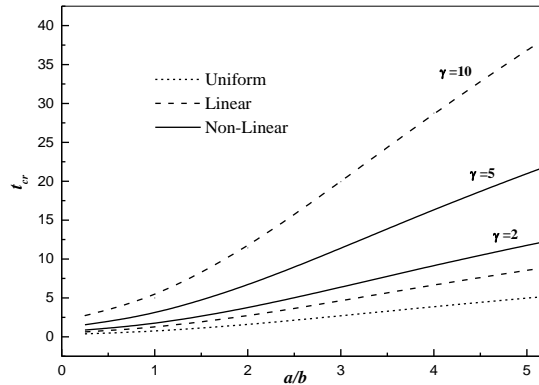


Fig. 5 Critical buckling temperature difference t_{cr} due to uniform, linear and non-linear temperature rise across the thickness versus the aspect ratio a/b and for different values of the non-linearity parameter γ . ($k=5$ and $a/b=10$)

6. Conclusions

In the present study, thermal buckling behavior of functionally graded plates subjected to uniform, linear and non-linear temperature rises across the thickness direction has been investigated on the basis of an efficient sinusoidal shear deformation theory. By dividing the transverse displacement into bending and shear components, the number of unknowns and governing equations of the present theory is reduced to four and is therefore less than alternate theories. The mechanical properties of the plate have been assumed to vary through the thickness of the plate as a power function. The neutral surface position for such plates has been determined. A good correlation has been observed between the present results and the available data in literature. Several parametric studies have been performed to show the effects of aspect ratio, plate thickness, thermal loading and also power law index on the critical buckling temperature of functionally graded rectangular plate. Finally, it can be said that the proposed higher order shear deformation theory is not only accurate but also provides an elegant and easily implementable approach for simulating thermal buckling behavior of FG plates. The formulation lends itself particularly well to finite element simulations (Curiel Sosa *et al.* 2013) and also other numerical methods employing symbolic computation for plate bending problems (Rashidi *et al.* 2012), which will be considered in the near future.

References

- Abrate, S. (2008), "Functionally graded plates behave like homogeneous plates", *Composites Part B: Engineering*, **39**(1), 151-158.
- Bodaghi, M. and Saidi, A.R. (2011), "Thermoelastic buckling behavior of thick functionally graded rectangular plates", *Archive of Applied Mechanics*, **81**, 1555-1572.
- Bouazza, M., Tounsi, A., Adda-Bedia, E.A. and Megueni, A. (2010), "Thermoelastic stability analysis of functionally graded plates: An analytical approach", *Computational Materials Science*, **49**, 865-870.

- Bouremana, M., Houari, M.S.A., Tounsi, A., Kaci, A. and Adda Bedia, E.A. (2013), "A new first shear deformation beam theory based on neutral surface position for functionally graded beams", *Steel and Composite Structures*. (in press)
- Bousahla, A.A., Houari, M.S.A., Tounsi, A. and Adda Bedia, E.A. (2013), "A novel higher order shear and normal deformation theory based on neutral surface position for bending analysis of advanced composite plates", *International Journal of Computational Methods*. (in press)
- Curiel Sosa, J.L., Anwar Bég, O. and Liebana Murillo, J.M. (2013), "Finite element analysis of structural instability using a switching implicit-explicit technique", *Int. J. Comp. Methods Eng. Sci. Mechanics*. (in press)
- Ganapathi, M. (2006), "Thermal buckling of simply supported functionally graded skew plates", *Composite Structures*, **74**, 247-50.
- Ibrahim, H.H., Tawfik, M. and Al-Ajmi, M. (2007), "Thermal buckling and nonlinear flutter behavior of functionally graded material panels", *Journal Aircraft*, **44**, 1610-8.
- Javaheri, R. and Eslami, M.R. (2002a), "Thermal buckling of functionally graded plates", *AIAA Journal*, **40**, 162-9.
- Javaheri, R. and Eslami, M.R. (2002b), "Thermal buckling of functionally graded plates based on higher order theory", *J. Therm. Stress.*, **25**(1), 603-625.
- Kazerouni, S.M., Saidi, A.R. and Mohammadi, M. (2010), "Buckling Analysis of Thin Functionally graded Rectangulare Plates with Two Opposite Edges Simply Supported", *International Journal of Engineering Transactions B: Applications*, **23**, 179-192.
- Kettaf, F.Z., Houari, M.S.A., Benguediab, M. and Tounsi, A. (2013), "Thermal buckling of functionally graded sandwich plates using a new hyperbolic shear displacement model", *Steel and Composite Structures*, **15**(4), 399-423.
- Khalfi, Y., Houari, M.S.A. and Tounsi, A. (2013), "A refined and simple shear deformation theory for thermal buckling of solar functionally graded plates on elastic foundation", *International Journal of Computational Methods*. (in press)
- Lanhe, W. (2004), "Thermal buckling of a simply supported moderately thick rectangular FGM plate", *Composite Structures*, **64**, 211-218.
- Matsunaga, H. (2009), "Thermal buckling of functionally graded plates according to a 2D higher-order deformation theory", *Composite Structures*, **90**, 76-86.
- Morimoto, T., Tanigawa, Y. and Kawamura, R. (2006), "Thermal buckling of functionally graded rectangular plates subjected to partial heating", *International Journal of Mechanical Sciences*, **48**(9), 926-37.
- Na, K.S. and Kim, J.H. (2004), "Three-dimensional thermal buckling analysis of functionally graded materials", *Composites Part B*, **35**, 429-37.
- Najafzadeh, M.M. and Heydaru, H.R. (2004), "Thermal buckling of functionally graded circular plates based on higher order shear deformation plate theory", *European Journal of Mechanics A/Solids*, **23**, 1085-100.
- Ould Larbi, L., Kaci, A., Houari, M.S.A. and Tounsi, A. (2013), "An efficient shear deformation beam theory based on neutral surface position for bending and free vibration of functionally graded beams", *Mechanics Based Design of Structures and Machines*, **41**, 421-433.
- Rashidi, M.M., Shoostari, A. and Anwar Bég, O. (2012), "Homotopy perturbation study of nonlinear vibration of Von Kármán rectangular plates", *Computers and Structures*, **106/107**, 46-55.
- Saidi, A.R. and Jomehzadeh, E. (2009), "On analytical approach for the bending/stretching of linearly elastic functionally graded rectangular plates with two opposite edges simply supported", *Proc. IMechE, Part C: Journal of Mechanical Engineering Science*, **223**, 2009-2016.
- Shariat, BAS., Eslami, M.R. (2005), "Effect of initial imperfections on thermal buckling of functionally graded plates", *Journal of Thermal Stresses*, **28**, 1183-98.
- Sohn, K.J. and Kim, J.H. (2008), "Structural stability of functionally graded panels subjected to aero-thermal loads", *Composite Structures*, **82**, 317-25.
- Suresh, S. and Mortensen, A. (1998), *Fundamentals of Functionally Graded Materials*, IOM

Communications Ltd., London.

- Yaghoobi, H. and Feraidoon, A. (2010), "Influence of neutral surface position on deflection of functionally graded beam under uniformly distributed load", *World Applied Sciences Journal*, **10**(3), 337-341.
- Zenkour, A.M. and Mashat, D.S. (2010), "Thermal buckling analysis of ceramic-metal functionally graded plates", *Natural Sciences*, **2**, 968-978.
- Zhang, D.G. and Zhou, Y.H. (2008), "A theoretical analysis of FGM thin plates based on physical neutral surface", *Computational Materials Science*, **44**, 716-720.